Advances in Applied Energy 6 (2022) 100094

Contents lists available at ScienceDirect

Advances in Applied Energy

journal homepage: www.elsevier.com/locate/adapen

Impact of model predictive control-enabled home energy management on large-scale distribution systems with photovoltaics

Hongyu Wu [a,*], Annabelle Pratt [b], Prateek Munankarmi [b], Monte Lunacek [b], Sivasathya Pradha Balamurugan [b], Xuebo Liu [a,b], Paul Spitsen [c]

[a] Mike Wiegers Department of Electrical and Computer Engineering, Kansas State University, Manhattan, Kansas 66506, USA
[b] National Renewable Energy Laboratory, 15013 Denver West Parkway, Golden, Colorado 80401, USA
[c] Department of Energy Office of Energy Efficiency and Renewable Energy, 1000 Independence Ave. SW, Washington DC 20585, USA

ARTICLE INFO

Keywords:
Home energy management system
Model predictive control
Stochastic optimization
Co-simulation
Photovoltaic
Electric vehicle

ABSTRACT

Residential customers use more than one-quarter of the electricity in the world. Optimally managing home energy consumption is an effective way of easing the operational challenges facing the electric grid with increasing solar photovoltaics (PV). This paper studies the impact of the future proliferation of home energy management systems (HEMS) in the presence of PV on large-scale distribution systems. First, we present a stochastic HEMS model that minimizes residential customers' thermal discomfort and energy costs under uncertainty. The HEMS model schedules the optimal operations of residential appliances in the presence of PV within a mixed-integer linear programming-based model predictive control framework that links the proposed HEMS to a quasi-steady-state time-series simulation tool. Extensive simulations are conducted for a stand-alone residential home using two tariff structures and for 1977 homes on an 8,500-node distribution feeder. Simulation results quantify the impact of the future proliferation of HEMS on the large-scale distribution system with PV.

1. Introduction

In 2021, more than one-quarter of the electricity in the world is consumed in the residential sector [1]. A home energy management system (HEMS) is one of the most effective tools to monitor the energy usage of smart appliances and subsequently sending the control commands to each controllable appliance for energy cost savings and peak load reduction.

HEMS related research has been focused on developing algorithms and mathematical approaches to effectively reduce peak demand, energy charges, and the carbon footprint of residential buildings while maintaining an acceptable level of comfort for the occupants [2]. A couple of deterministic optimization models have been studied. An energy scheduling model was presented in [3], in which residential consumers optimally schedule their electricity consumption, generation, and storage in a dynamic pricing environment. An intelligent heating and air-conditioning scheduling method was proposed in [4] to address customer convenience and energy cost while considering the characteristics of the thermal appliances. In [5], an efficient power scheduling scheme for electric appliances was determined by combining real-time electricity pricing and inclining block rates; the proposed approach reduced both the electricity cost and the peak-to-average ratio. In [6], response fatigue phenomenon was considered in HEMS models to prevent consumers from getting tired of making decisions based on different tariffs and electricity usage. A HEMS-based, real-time control system that controls the schedules of appliances for demand response was proposed in [7]. An approximate dynamic programming algorithm was proposed in [8,9] to solve the HEMS problem with significant improvement in computation time while maintaining acceptable solution accuracy. In [10], a human-centric smart HEMS that integrates ubiquitous sensing data from the physical and cyber layers to discover the patterns of power usage and cognitively understand the behavior of residents was proposed. In [11], recent studies on residential building energy management were reviewed. It has been found that building energy management can help the grid improve stability by optimizing flexible loads as a result of the advanced technologies of smart sensing, smart metering, smart appliances, electric vehicles and energy storage. In [12], a multi-objective, multi-scale, mixed integer linear programming (MILP) based multi-energy management system was proposed to optimally determine the operation of a mix of electric vehicles and battery energy storage systems for greenhouse gas mitigation. The model was evaluated in five types of residential buildings in Switzerland.

A wide variety of approaches has also been proposed to deal with uncertainty in HEMS optimization. Uncertainties in real-time electricity prices were considered in the residential appliance scheduling problem

* Corresponding author.
E-mail address: hongyuwu@ksu.edu (H. Wu).

https://doi.org/10.1016/j.adapen.2022.100094
Received 1 March 2022; Received in revised form 13 April 2022; Accepted 14 April 2022
Available online 18 April 2022

Nomenclature

NT	Number of time periods
NS	Number of scenarios
T_B, T_L	Binding and look-ahead time periods in MPC
Pr_s	Occurrence probability of scenario s
$p^{grid}_{t,s}$	Power from grid at time t in scenario s
$\Theta^{\min}_{i,t}, \Theta^{\max}_{i,t}$	Min/max substance temperature set point for appliance i at time t, $i \in$ {hvac,wh}
$\Theta^{desired}_{i,t}$	Desired substance temperature controlled by appliance i at time t, $i \in$ {hvac,wh}
τ	Time interval, in hours
$\varphi^{(\cdot)}_{(\cdot)}$	Thermal coefficients
$slope_{i,t}$	Penalty factor of appliance i for substance temperature deviation from the desired temperature
$QC^{\min}_i, QC^{\max}_i$	Min/max charge power, $i \in$ {ev,bess}
$QD^{\min}_i, QD^{\max}_i$	Min/max discharge power, $i \in$ {ev,bess}
$SOC^{\min}_i, SOC^{\max}_i$	Min/max state of charge, $i \in$ {ev,bess}
Cap_i	Capacity, $i \in$ {ev,bess}
E^{req}_i	Estimated energy requirement to reach target SOC, $i \in$ {ev}
$\eta^{char}_i, \eta^{dischar}_i$	Charge/discharge efficiency, $i \in$ {ev,bess}
$Penalty_i$	EV penalty for insufficient energy at departure
λ_t	Electricity price at time t
$\hat{\Theta}^{out}_{t,s}$	Outdoor temperature at time t in scenario s
$\hat{\chi}_{t,s}$	Solar irradiance at time t in scenario s
$\hat{w}_{t,s}$	Hot water usage at time t in scenario s
$\hat{p}_{solar,t,s}$	Solar generation at time t in scenario s
$\hat{p}_{ncl,t,s}$	Noncontrollable loads at t in scenario s
$\theta_{i,t,s}$	Substance temperature of thermal appliance i at time t in scenario s
$\theta^{SP}_{i,t,s}$	Substance temperature set point of thermal appliance i at time t in scenario s
$p_{i,t,s}$	Electricity consumption (+) or generation (-) of appliance i at time t in scenario s
$SOC_{i,t,s}$	State of charge of appliance i at time t in scenario s
$Slack_{t,s}$	Nonnegative slack variable for EV energy requirement at time t in scenario s

in [13] by adopting a scenario-based Monte Carlo simulation. To capture the trade-off between the expected costs and the risk of exposure to uncertainties in the stochastic inputs, the conditional value-at-risk was used in [14] for the real-time scheduling of residential appliances in the HEMS. In [15], the monetary expense of the household was minimized by considering the uncertainties in the operation time of the appliances, the volatility in the renewable resources, the time-varying prices, and the comfort of the customers. The proposed approach adjusts the deterministic solution by using adaptation variables to accommodate the stochastic energy consumption patterns. An approach to modeling and optimizing home energy consumption by categorizing the classes of loads was proposed in [16], wherein several classes of demand-including heating, ventilating, and air-conditioning (HVAC); plug-in hybrid electric vehicles (EVs); and deferrable loads (e.g., washer and dryer) are considered; and a multi-scale, multistage, stochastic optimization framework was proposed to control these classes. The authors of [17] proposed dual decomposition into several subproblems and a stochastic gradient to handle the temporally coupled constraints in scheduling deferrable loads considering future price uncertainty; the price forecast error is mitigated using an online approach in a dynamic pricing environment. An uncertainty quantification approach was proposed in [18] to address the challenge of balancing highly stochastic demand with volatile energy supply characterized by renewable energy

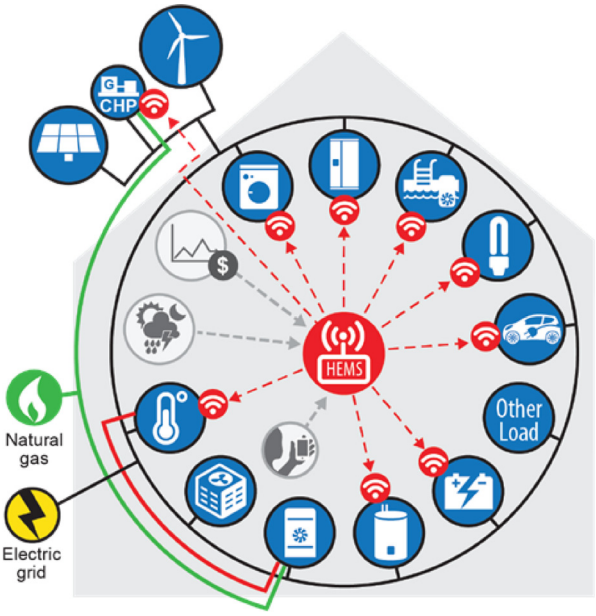

Fig. 1. Conceptual diagram of individual HEMS.

resources; here, the dependence of the cost of service on the volatility in demand is underlined, and a framework is proposed to mine the patterns in the distributions of energy demand to justify the choice of energy demand distribution signature in terms of the characteristics of the users. In [19], a two-stage stochastic optimization method was proposed to schedule a real-time, hydrogen-based vehicle for a multi-energy system including electrical power, natural gas, heating power, cooling power networks, and energy storage-coupled with different energy carriers from an economic point of view. An energy management system was developed in [20] to optimally schedule an electric water heater while considering the self-consumption of a residential PV installation with performance losses due to production uncertainties.

These works used various methods to show modeling improvements on handling uncertainties or to underline theoretical advancements in solutions compared to previous algorithms; however, only a few of these models were evaluated in a large-scale distribution feeder. It is still under-researched how the future proliferation of HEMS would affect the distribution system with solar PV.

This paper aims to fill the gap by using a stochastic HEMS within a model predictive control (MPC) framework [21] to demonstrate the potential impact of HEMS in large-scale distribution systems. The HEMS decides the optimal operational schedules of residential appliances in the presence of PV, as illustrated in Fig. 1, based on price and weather inputs. Extensive simulations linking the proposed HEMS to a quasi-steady-state time-series (QSTS) simulation tool are conducted in a smart residential home using two tariff structures and on an 8,500-node distribution feeder with 1977 smart homes with diverse comfort settings. The conceptual diagram of the distribution system is illustrated in Fig. 2, in which homes with HEMS are connected to each of the three phases of the feeder. Real-time communications to weather and energy price forecasts enable the HEMS to look into the future and optimally meet the residential customers needs. The contributions of this paper are threefold:

1) Stochastic scheduling models for home appliances were extensively studied in the literature [21–24]. however, existing models rarely include high-fidelity and realistic representations of residential home and appliance models to demonstrate HEMS algorithms. This work expands upon prior work [2,25] by incorporating stochastic HEMS [21] into high-fidelity residential home models that explicitly model the thermal envelope, air conditioner, EV, and water heater. Much finer-

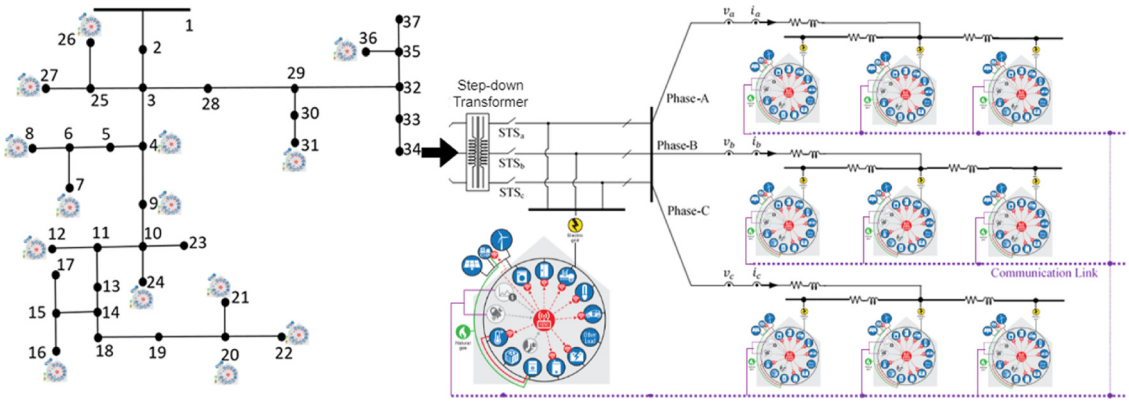

Fig. 2. Conceptual diagram of integrating HEMS in a distribution feeder.

granularity modeling details of the thermal envelope and appliances than those in the literature allow for a more accurate assessment on the impact of the stochastic HEMS on distribution feeders.

2) A co-simulation framework is developed to integrate the stochastic HEMS by leveraging National Renewable Energy Laboratory's (NREL's) Integrated Energy System Model (IESM) framework [25] to include a larger number of homes on a realistic distribution feeder. The IESM integrates the simulation of DERs (including PV and battery systems), a distribution feeder, buildings (including building appliances and building thermal performance), and HEMS under different markets or tariff structures through a co-simulation coordinator. The integration of the stochastic HEMS and the IESM provides the ability to assess an accurate impact of HEMS on the physical performance of a large-scale distribution feeder.

3) We evaluate the impacts of HEMS managing EVs, battery energy storage systems (BESS), air conditioners, and water heaters in the presence of PV. We conduct the co-simulation on an IEEE 8,500-node feeder with 1977 homes. This paper builds on prior work [2,25]—by considering a more complex HEMS algorithm that controls multiple residential appliances—to provide insights into the expected performance of a portfolio of households with both rooftop PV systems and multiple controllable consumer technologies in a large-scale distribution feeder.

The rest of the paper is organized as follows. The mathematical formulation of the HEMS model is provided in Section 2. The MPC framework and co-simulation platform are described in Section 3. Extensive simulation results are presented and analyzed in Section 4. The conclusions are made in Section 5.

2. HEMS model

2.1. Objective function

The details on the stochastic HEMS model [21], including the objective functions and associated constraints, are presented in this section. We consider the following functions, which are used to describe the constraints for and the needs of the end users, typically utilities and/or residential customers:

1. Thermal discomfort, which is represented by a linear penalty function (1) for temperature deviation between the predicted value and the customer's desired temperature [26]:

$$J_1 = \sum_{s=1}^{NS} Pr_s \cdot \sum_{i\in\{hvac,wh\}} \sum_{t=1}^{NT} slope_{i,t} \cdot \left|\Theta_{i,t}^{desired} - \theta_{i,t,s}\right| \tag{1}$$

2. Total energy cost ($), which represents the cost of electricity and the cost of battery degradation (2). Time-based pricing schemes, including dynamic and time-of-use (TOU) pricing, could be applied to the stochastic optimization model:

$$J_2 = \sum_{s=1}^{NS} Pr_s \cdot \sum_{t=1}^{NT} \tau \cdot (p_{t,s}^{grid} \cdot \hat{\lambda}_{t,s} + c_{t,s}^{bd}) \tag{2}$$

A combination of these two objectives through a weighted average becomes the overall objective function (3):

$$\begin{aligned} Minimize \quad & J = \alpha_1 \cdot J_1/\tilde{J}_1 + \alpha_2 \cdot J_2/\tilde{J}_2 \\ & + \textstyle\sum_{i\in\{ev\}} \sum_{s=1}^{NS} Pr_s \cdot Penalty_i \cdot Slack_{i,s} \end{aligned} \tag{3}$$

where $\tilde{J}_1, \tilde{J}_2$ are the upper bounds of the corresponding objective components from (1)–(2), which are estimated by a computationally efficient method in a preprocessing stage to combine different objective components. Specifically, if the user-specified preference is identified as a two-objective optimization, the deterministic model with the forecasted time series is run with the integer variables relaxed, and the resulting optimization problem is solved by using linear programing. The objective of the first deterministic run is to minimize the total energy cost such that the upper bound of the thermal discomfort, i.e., $\tilde{J}_2$, is obtained. The solution time of this run is trivial because a linear programing problem of a single scenario is solved. Then the deterministic model is executed again with the objective of minimizing the thermal discomfort such that the upper bounds of other objective components are determined. The solution time for the second run is also minimal because another deterministic linear programing problem is solved. By executing the relaxed deterministic models twice with negligible computational effort, good estimates of the upper bound for each objective component can be procured according to our numerical experiences.

Slack variables are introduced into (3) to provide the HEMS with more flexibility by allowing some constraints to be violated at an extremely high penalty cost; the third line in (3) reflects these penalty costs. The proposed stochastic optimization model minimizes the weighted average of multiple objective components while aiming to satisfy the operational constraints described in the next subsection. In addition to the weighted average of multiple objective components, another approach to handle the proposed multi-objective optimization problem is to obtain a Pareto front; however, this approach is not widely applied in the home energy management since another criterion is still required to select the final appliance schedule from all Pareto efficient solutions. On the other hand, the relative weights of the objective components can be straightforwardly derived from the user preference survey, for example, by using the Simple Multi-Attribute Rating Technique Exploiting Ranks (SMARTER) method [27].

2.2. HEMS constraints

2.2.1. House-level constraints

The home-level power balance constraint is listed in (4). Constraint (4) guarantees that the electricity generation and load are balanced at

time t, where $p_{t,s}^{grid}$ is positive when the house extracts electricity from the grid and negative when the house injects electricity into the grid, and $\hat{p}_{ncl,t,s}$ is the noncontrollable load. Here, the scheduled power consumption/generation at each time interval is the average value during a given time interval:

$$p_{t,s}^{grid} + \hat{p}_{solar,t,s} = \sum_{i \in A} p_{i,t,s} + \hat{p}_{ncl,t,s}, \ \forall t, \forall s \tag{4}$$

2.2.2. HVAC

A first-order linear thermodynamic model, i.e., 1R1C model, is used to describe the evolution of the room temperature as a function of the power consumed by the HVAC, outdoor temperature, and solar irradiance. The HVAC constraints are listed as follows:

$$\Theta_{hvac,t}^{\min} \le \theta_{hvac,t}^{SP} \le \Theta_{hvac,t}^{\max}, \forall t \tag{5}$$

$$\theta_{t,s}^{in} = \begin{cases} \varphi^{rm}\theta_{t-1,s}^{in} + \varphi_{hvac}^{c} p_{hvac,t,s} + \varphi_{si}\hat{\chi}_{t,s} + \varphi^{out}\hat{\Theta}_{t,s}^{out} \\ \qquad\qquad\qquad\qquad\qquad\qquad\qquad\qquad \text{if cooling} \\ \varphi^{rm}\theta_{t-1,s}^{in} + \varphi_{hvac}^{h} p_{havc,t,s} + \varphi_{si}\hat{\chi}_{t,s} + \varphi^{out}\hat{\Theta}_{t,s}^{out} \\ \qquad\qquad\qquad\qquad\qquad\qquad\qquad\qquad \text{if heating} \end{cases} \tag{6}$$

Constraint (5) shows that the cooling or heating set points should be within their respective ranges, as prescribed by the residential customer. Constraint (6) represents the thermal dynamics of the room temperature in both cooling (c) and heating (h) modes, wherein a combined heat and power (CHP) heating contribution is included in heating mode. The heating or cooling mode, known a priori to the model, is selected by the residential customers. Here, the cooling or heating set points are the only decision variables of the HVAC; other variables, such as the ON/OFF status and power consumption, are associated with the set points in the proposed HEMS.

2.2.3. Water heater

The operational constraints of the water heater, listed in (7) and (8), are similar to the HVAC constraints, but they consider terms for forecasted hot water usage and CHP heat contribution:

$$\Theta_{wh,t}^{\min} \le \theta_{wh,t}^{SP} \le \Theta_{wh,t}^{\max}, \forall t \tag{7}$$

$$\theta_{t,s}^{wh} = \varphi_{wh}^{tmp}\theta_{t-1,s}^{wh} + \varphi_{wh}^{usg}\hat{w}_t + \varphi_{wh} p_{wh,t,s} + \varphi_{wh}^{out}\hat{\Theta}_{t,s}^{out} \quad \forall t, \forall s \tag{8}$$

Analogously, the heating set point of the water heater is the decision variable, whereby its ON/OFF status and power consumption are determined. Here, the heating or cooling set points of the HVAC, refrigerator, and water heater are constrained within the user-specified upper and lower bounds of the substance temperature, whereas the substance temperatures are allowed to go beyond the upper and lower bounds.

2.2.4. Battery-related appliances considering degradation

The BESS and EV constraints include the charging and discharging rate limits, state-of-charge (SOC) dynamics, SOC limits, and energy requirement, which are given in (9)–(12), respectively. In (9), is positive when charging, negative when discharging, and zero when the storage is idling. Constraint (12) is applied only to EV, which ensures that the EV's energy requirement is satisfied or can be relaxed with a high penalty:

$$p_{i,t,s} \in \{0, [-QD_i^{\max}, -QD_i^{\min}], [QC_i^{\min}, QC_i^{\max}]\} \quad i \in \{ev, bess\}, \forall t, \forall s \tag{9}$$

$$SOC_{i,t,s} = \begin{cases} SOC_{i,t-1,s} + p_{i,t,s} \cdot \eta_i^{char}/Cap_i, \ p_{i,t,s} > 0 \\ SOC_{i,t-1,s} + p_{i,t,s}/\eta_i^{dischar}/Cap_i, \ p_{i,t,s} < 0 \end{cases} \tag{10}$$

$$SOC_i^{\min} \le SOC_{i,t,s} \le SOC_i^{\max}, \ i \in \{ev, bess\}, \forall t, \forall s \tag{11}$$

$$\sum_{t \in T^i} p_{i,t,s} \cdot \tau + Slack_{i,s} \ge E_i^{req}, i \in \{ev, bess\}, \forall s \tag{12}$$

The EV's energy requirement can be estimated by calculating the difference between the arrival and departure SOC. To calculate the energy requirement in the MPC-based approach, five charging cases are considered, each of which represents one possible correlation among initial, arrival, and departure SOC. In addition, the estimated costs of the battery degradation are captured through a linearization of the model proposed in [28], which estimates both energy capacity fade and power fade and includes effects caused by temperature (T), average SOC, and depth of discharge (DoD). The battery degradation cost, $c_{t,s}^{bd}$, calculated in (13), is added in the energy cost component in the overall objective function (2):

$$c_{t,s}^{bd} = \mathbf{max}\Big\{(c_{t,s}^{Q,T} + c_{t,s}^{Q,SOC} + c_{t,s}^{Q,DOD}), \\ (c_{t,s}^{P,T} + c_{t,s}^{P,SOC} + c_{t,s}^{P,DOD})\Big\} \tag{13}$$

where $c_{t,s}^{Q,T}$, $c_{t,s}^{Q,SOC}$, and $c_{t,s}^{Q,DOD}$ are the capacity-fade costs associated with temperature, SOC, and DOD, respectively. $c_{t,s}^{P,T}$, $c_{t,s}^{P,SOC}$, and $c_{t,s}^{P,DOD}$ are the power-fade costs associated with temperature, SOC, and DOD, respectively. More details about the definition and the calculation of each term in (13) can be found in [28]. Other appliances—such as dishwasher, clothes washer and dryer, pool pump, and micro-CHP—can be integrated into the HEMS model as described in [21]. A stochastic optimization model for the optimal schedules of residential appliances is formulated in (1)–(13) as an MILP problem.

3. Proposed co-simulation framework

3.1. Uncertainty representation

The proposed stochastic optimization model uses scenarios for representing uncertainties, which can include outdoor temperature, PV generation, hot water usage, and noncontrollable load. The probability distribution functions of the uncertainties for those parameters are inputs to the HEMS. The uncertainties can be characterized by an autoregressive moving average (ARMA) [29]. Because the autocorrelation factor of the time series would decrease dramatically as the time lag increases, the forecast error is represented by a lower-order ARMA (1,1) as follows:

$$X_t = \alpha \cdot X_{t-1} + \beta \cdot Z_{t-1} + Z_t \tag{14}$$

The ARMA constants are acquired by minimizing the root-mean-square-error between the simulated ARMA time series and the measured data [30]. For simplicity, the ARMA constants in this work are assumed to follow a truncated normal distribution function with a standard deviation equal to a certain percentage of the forecast; however, different probability distributions can also be used to represent heterogeneous uncertainty components. The ARMA model adopted provides a parsimonious description of a stationary stochastic process for statistical forecasts of time series. To improve the efficiency of the Monte Carlo sampling over a high dimension of uncertainty space, a low-discrepancy method, Latin hypercube sampling (LHS), is used to generate evenly distributed random samples with smaller variance [31].

Scenario-reduction techniques are used to find a trade-off between computational speed and accuracy. The scenario-reduction method determines a scenario subset of the prescribed cardinality and a probability measure based on this subset that is closest to the initial distribution in terms of a probability metric [32]. Scenario-reduction algorithms include the fast backward method, the fast backward/forward method, and the fast backward/backward method [32]. The algorithms have different computational performance and accuracy, so the selection of an algorithm depends on the size of the problem and the required solution accuracy. The forward method is adopted here because the number of reduced scenarios is small (strong reduction).

3.2. MPC

MPC is a method of process control while satisfying a set of constraints. It optimizes a finite time horizon, but it only implements the current timeslot and then optimizing again, repeatedly. Based on the principle of MPC, the proposed stochastic optimization model is described in Algorithm 1:

Algorithm 1 MPC-Based Stochastic HEMS.

Step 1. At time t, gather updated forecast data: $\hat{\lambda}_{t,0}$, $\hat{\Theta}^{out}_{t,0}$, $\hat{w}_{t,0}$, $\hat{p}_{solar,t,0}$, $\hat{p}_{ncl,t,0}$, $\forall t \le T_B + T_L$; get initial status: $\bar{p}_{i,0}$, $\forall i \notin hvac, wh$ and $\bar{\theta}_{i,0}$, $\forall i \in hvac, wh$ from the QSTS simulation tool.

Step 2. Preprocess the multi-objective of the user preferences. Generate scenarios by using LHS, and further reduce the number by using scenario reduction methods.

Step 3. Run the proposed stochastic HEMS model to obtain optimal appliance schedules and set points, i.e., $\bar{p}^{*}_{i,t}, \bar{\theta}^{SP*}_{i,t}, \forall t \in T_B$ and $\bar{p}^{*}_{i,t,s}, \bar{\theta}^{SP*}_{i,t,s}, \forall t \in T_L$.

Step 4. Pass $p_{i,t} = \bar{p}^{*}_{i,t}$,and $\theta^{SP}_{i,t} = \bar{\theta}^{SP*}_{i,t}, \forall t \in T_B$ to the QSTS simulation tool, and run the QSTS simulation.

Step 5. Let $t = t+1$; go back to **Step** 1 until $t = NT$.

Remarks:

1. It is imperative to identify decisions made by the MPC-based HEMS. Here, the decisions associated with binding intervals i.e., T_B are implemented. In contrast, the decisions pertaining to the look-ahead (advisory) intervals-i.e., T_L-are scheduled but not implemented. For example, at 08:00, the HEMS optimally schedules the operation of appliances for the entire schedule horizon-e.g., the next 12 hours-but the dispatch points scheduled from 08:00 to 08:05 are implemented, and this process repeats every 5 minutes. The frequency of running the MPC-based HEMS as well as the length of the binding and look-ahead time intervals are entirely configurable.
2. The forecast errors in pricing, outside temperature, PV generation, hot water usage, and noncontrollable load can be mitigated by two means: *i*) the MPC-based approach, which incorporates predictive or measured values—this approach is somewhat similar to the approach used by system operators in bulk power systems where a production cost model is continuously solved in a real-time market (e.g., every 5 minutes) with the latest information to avoid large forecasting errors; and *ii*) the stochastic optimization, which, by its nature, is capable of dealing with forecast errors and making an optimal decision under uncertainty. The use of an MPC-based approach combined with the stochastic optimization to manage the uncertainty facing a residential customer constitutes another contribution of this paper.

3.3. QSTS co-simulation

To demonstrate the impact of HEMS on future smart cities, we first develop a co-simulation framework that couples the HEMS decision making to a GridLAB-D simulation of a single house. GridLAB-D is a power distribution system simulation tool developed by the Pacific Northwest National Laboratory [33]. It performs QSTS simulations of distribution feeders and homes and uses agent-based methods to simulate end-use loads, such as appliances and heating/cooling systems. It also provides retail market modeling tools, including price-responsive end-use loads. Fig. 3 shows the HEMS and GridLAB-D simulation for a single house. Consumer preferences, such as the objective function weights and desired set point profiles, are inputs to the HEMS. Price and weather data are provided to both the HEMS and the house simulation. The HEMS optimizes the appliance set points during the whole scheduling horizon and outputs the set points for the next time period—i.e., binding decisions—to GridLAB-D, which uses them to calculate appliance power and customer utility values, such as indoor air temperature and battery SOC. These values are provided as inputs to the HEMS for the next optimization.

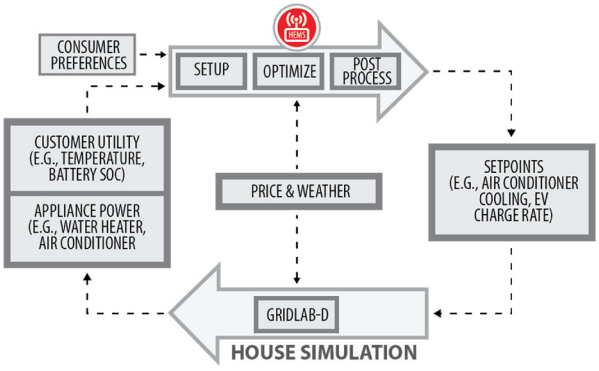

Fig. 3. QSTS simulation flowchart for a single house.

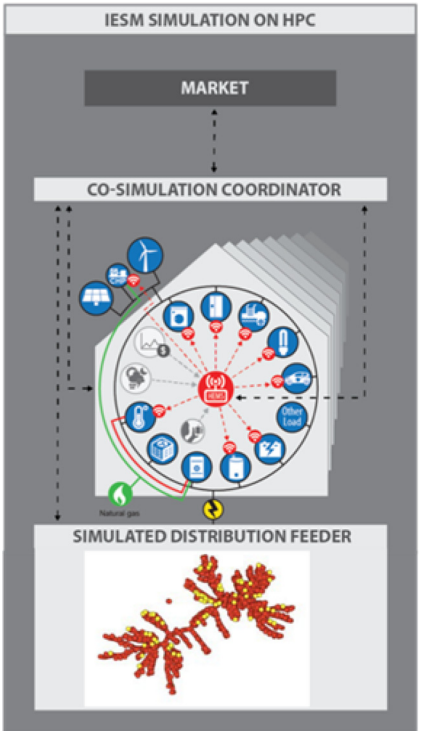

Fig. 4. Diagram of the IESM, including a co-simulation coordinator, simulated distribution feeder, simulated homes with HEMS, and markets.

To include a larger number of homes on a realistic distribution feeder, we further integrated the HEMS with the houses using a modified version of NREL's IESM simulation framework [25], as shown in Fig. 4. The IESM integrates the simulation of a distribution feeder, DERs (including PV and battery systems), buildings (including building appliances and building thermal performance), and HEMS under different markets or tariff structures through a co-simulation coordinator coded in Python [34].

The co-simulation coordinator is responsible for the data exchange between various components and the timing of the execution of all the components with different time steps. The coordinator interfaces with the building and distribution feeder simulations, the HEMS, and the market that sets the different tariff structures. The different components of the simulation are described in more detail in [34]. The simulations are performed using high-performance computing to accommodate hundreds of HEMS using an MPC approach.

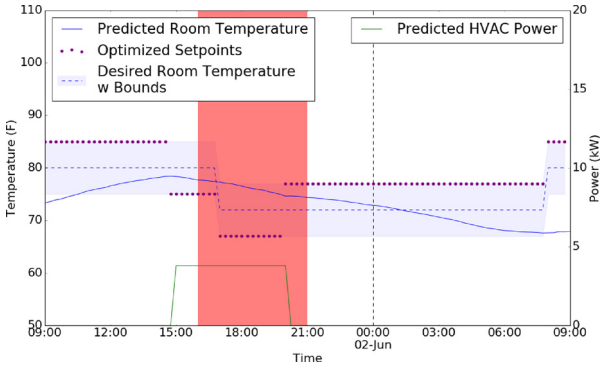

Fig. 5. Optimized cooling set points and predicted room temperature and HVAC power for 24 hours generated by HEMS at 9:00 a.m. on June 1.

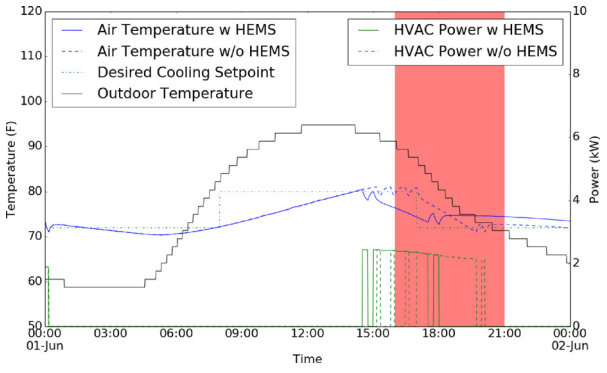

Fig. 6. Simulation results for the air conditioner for June 1.

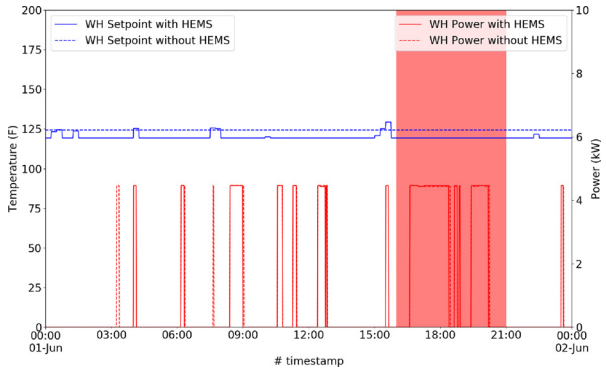

Fig. 7. Simulation results for the water heater for June 1.

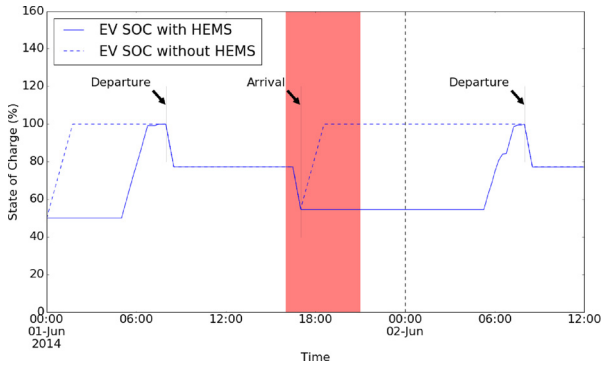

Fig. 8. Simulation results for the EV. The figure shows June 1, and the morning of June 2, 2014.

4. Simulation results

4.1. Simulations on a single home

We present a case study wherein the HEMS optimizes the cooling set point for the air conditioner, the EV charging rate, and the heating set point for the water heater; therefore, the thermal envelope, the air conditioner, the EV, and the water heater are modeled explicitly in GridLAB-D. Other loads are collectively represented as a ZIP load [33]. We use equal weights in the objective function for energy cost and thermal discomfort.

The HVAC parameters used within the MPC were obtained by applying linear regression to data obtained from a GridLAB-D simulation of the house without the HEMS. The GridLAB-D simulation for the HVAC parameters was conducted using different indoor temperature set points, outside temperature, and solar irradiance with a fixed HVAC set point. We used weather data from the city of Fresno, California, for both the house simulation and the weather forecast input for the HEMS. We performed simulations as follows:

4.1.1. Single-tariff simulations

The first tariff we adopted is the ETOU-B plan, which is used by Pacific Gas & Electric Company (PG&E) [35], where the peak price of $0.356/kWh is applied from 16:00–21:00 (4:00 p.m.–9:00 p.m.), and the off-peak price of $0.2529/kWh is applied the rest of the day. Figs. 5–8 show results from a simulation that ran for a 24-hour period with a 1-minute granularity. The HEMS optimization was performed every 15 minutes using a 24-hour time horizon. The shaded regions in all figures represent the peak price periods.

Fig. 5 shows the prediction variables that the HEMS used to make its decision at 9:00 a.m. on June 1. The predicted HVAC power consumption solved by the HEMS model is shown in green. As shown, the HEMS precooled before the peak pricing period and followed the customer's desired room temperature as well as the bounds of their preference.

The room temperatures are shown in Fig. 6 for the optimized case (with HEMS) and the nonoptimized case (without HEMS), along with the customer's desired temperature profile, the outdoor temperature, and the HVAC power consumption for the same day. Results for the nonoptimized case are obtained by setting the cooling set points equal to the customer's desired temperature.

The initial indoor air temperature in the house was set to 72°F, and it increased as the outdoor temperature increased. It was assumed that the house was not occupied during the day; therefore, the desired cooling set point was increased to 80°F between 8:00 a.m.–05:00 p.m. Fig. 5 shows that during the early hours of the morning, when the room temperature was lower than the desired comfort temperature, the HVAC did not turn on. We can see that, given the same initial conditions, the room temperature with a HEMS was initially similar to that without a HEMS. At 02:00 p.m., the HEMS turned on the HVAC to precool the house. This increased the air-conditioner power before the peak price period and decreased it during the peak price period to minimize the cost while maintaining customer comfort.

Figure 7 shows the heating set point and electricity consumption of the water heater. As shown, the HEMS preheated before the peak pricing period and followed the customer's desired hot water temperature as well as the bounds of their preference.

Figure 8 depicts the SOC of the EV with and without the HEMS. The initial SOC was set to 50%. The sharp changes in SOC slightly after the arrivals and departures were a result of GridLAB-D's EV model, which applies the full discharge because of vehicle miles traveled at those times. Without the HEMS, the EV's battery is charged during peak hours, shortly after the vehicle arrives home. With the HEMS, charging is delayed until closer to departure to both reduce energy cost and limit battery degradation [28].

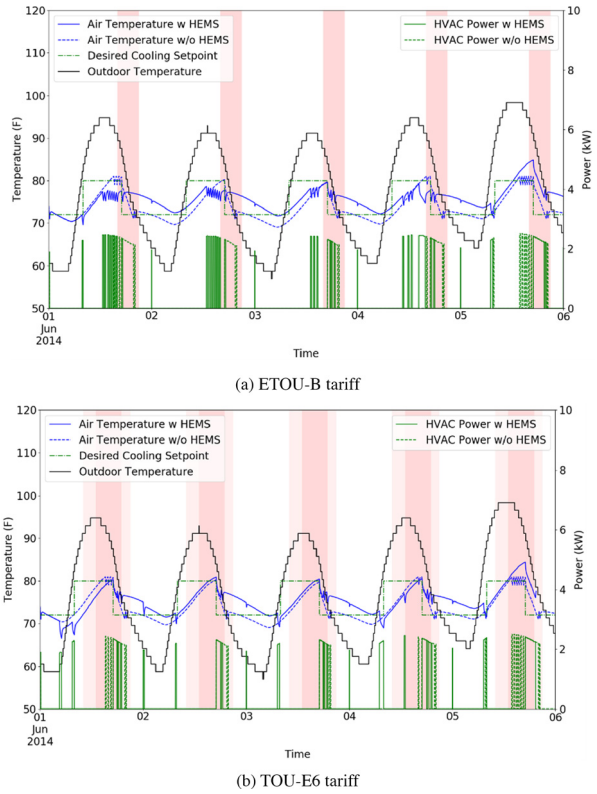

(a) ETOU-B tariff

(b) TOU-E6 tariff

Fig. 9. Comparison of HVAC simulation results for 5 days under different tariffs.

4.1.2. Two-tariff simulations

We evaluated the effectiveness of the proposed HEMS to handle different tariff structures through comparative simulations using both PG&E's ETOU-B and TOU-E6 plans [35]. For the TOU-E6 plan, rates are lowest in the morning and late evening during weekdays, with a peak price of $0.44/kWh applied from 13:00–19:00 (1 p.m.–7 p.m.), a partial peak price of $0.32/kWh from 10:00–13:00 (10 a.m.–1 p.m.) and 19:00–21:00 (7 p.m.–9 p.m.), and an off-peak price of $0.23/kWh applied the rest of the day. Fig. 9 compares the simulation results of the air conditioner for June 1–5 under the two different tariff structures considered. Under either tariff structure, shown in Fig. 9 (a) and (b), the HVAC behaved somewhat similarly for each of the five days when it precooled the house before the electricity price increased. The precooling before the peak price or partial-peak periods and then the reduction in power consumption during those periods could minimize cost while maintaining customer comfort.

As shown in the comparison of Fig. 9 (a) to (b), the HEMS consumed much more electricity during off-peak hours under the ETOU-B. This is because the outside temperature reached its peak during off-peak periods under ETOU-B. These results show that tariff structures affect the timing of and total demand for electricity when a HEMS is used. The proposed HEMS and MPC framework allow us to understand the impact of various tariff structures on end-use decisions made by energy management systems, which might be the first step toward a fundamental understanding of the physical performance of the distribution feeder and the market structures driving operations for the utilities.

4.2. Large-scale distribution feeder simulations

4.2.1. Simulation setup

We simulated in GridLAB-D an 8,500-node test feeder with 1977 homes that was created for the Transactive Energy Modeling and Simulation Challenge facilitated by the National Institute for Standards and Technology [36]. This feeder is used to represent a feeder in a hypothetical city. To mimic the diversity of the city, these house models have different combinations of attributes, such as square footage and insulation. All the homes have an air conditioner, but only 1013 of the homes have an electric water heater (the rest have natural gas water heaters). We modified the feeder model by randomly adding rooftop PV systems to 25%, i.e., 494, of the homes. The PV panels are sized based on the house square footage following the methodology described in [37], and the inverter ratings match the PV panel ratings. We also added BESS randomly to a subset of homes with PV. We aimed for a BESS penetration of 2%, resulting in 39 of the 494 homes that have a rooftop PV system receiving a BESS. All BESS are sized at 5 kW/13.5 kWh, based on commercially available residential battery systems.

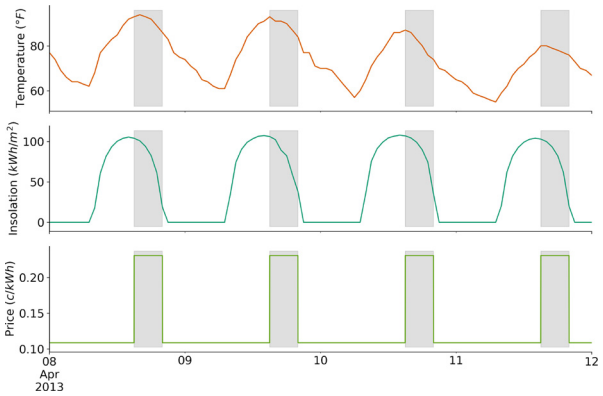

Fig. 10. Simulation inputs including outdoor temperature (top), solar insolation (second from top), and TOU rates (bottom).

We first simulate a baseline scenario with no HEMS and with the BESS in an idle mode, i.e., not charging or discharging, because some form of control is required to operate the BESS when it is active, which would set a more complicated baseline behavior to compare against. Then we simulate a price-responsive scenario with some of the homes coupled to a HEMS. We assigned the HEMS in a prioritized way such that all houses that have a BESS, rooftop PV, and an electric water heater received a HEMS. Next, we assign HEMS to houses with a BESS and rooftop PV, and finally to houses with an electric water heater. In total, 400 houses are coupled with a HEMS, resulting in a HEMS penetration of approximately 20%. The HEMS is set to run every 30 minutes and optimize based only on cost to simplify the analysis.

We use typical weather data for Phoenix, Arizona, for a full week in the spring for the month of April when air-conditioning use is high but not continuous, as would be the case on a typical summer day. The outdoor temperature, solar insolation, and TOU price are shown in Fig. 10. We use retail electricity rates that are currently in place for households in Arizona. The TOU rate has a varying electricity price with peak and off-peak rates. The summer peak and off-peak rates are 23.068 c/kWh and 10.873 c/kWh, respectively. Summer peak hours are from 3:00 p.m. to 8:00 p.m., Monday through Friday [38] and are indicated by the vertical grey bars in this and other figures. All weekend hours are off peak; therefore, we only simulated weekdays. For this study, we assume that the houses are compensated for exported power at the TOU rate.

The desired air and water temperature profiles are set to constant values. The desired temperatures for each house are different, varied uniformly between 70°F and 75°F for the air temperature and between 120°F and 140°F for the water temperature. A randomized water draw profile from [36] is used for each home. Each HEMS uses the MPC described in Section 3.2 to adjust the air and water temperature set points from the desired temperature to minimize the cost. The HEMS is allowed to adjust the air temperature set points up to 2.5°F above or below the desired air temperature and up to 10°F above or below the desired water temperature. This allows the air to be precooled and the water to be preheated before the peak electricity prices. The battery and SOC constraint are set to 50% in the HEMS.

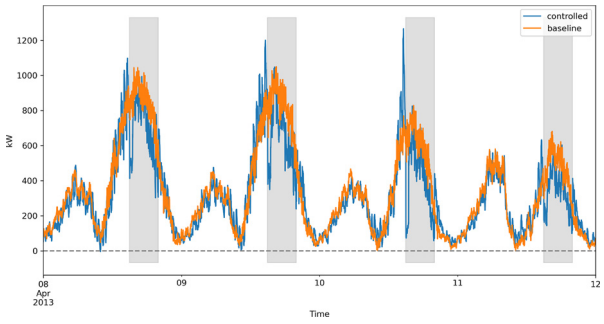

Fig. 11. Comparison of the total net power of only the homes that are coupled to HEMS in the controlled scenario.

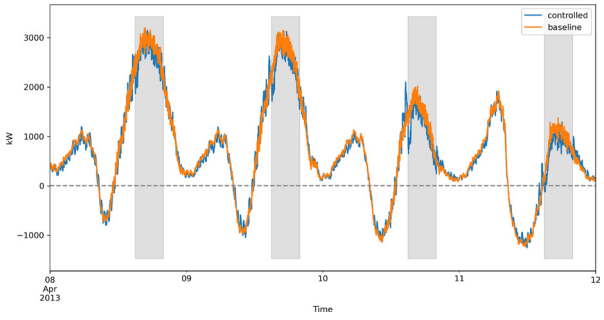

Fig. 12. Comparison of the total net power of all homes.

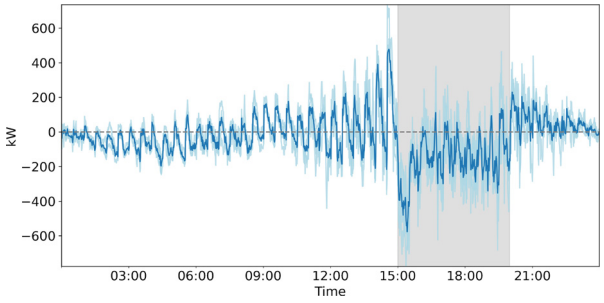

Fig. 13. Net power differences for each day (light blue) and average difference over all days (dark blue). (For interpretation of the references to colour in this figure legend, the reader is referred to the web version of this article.)

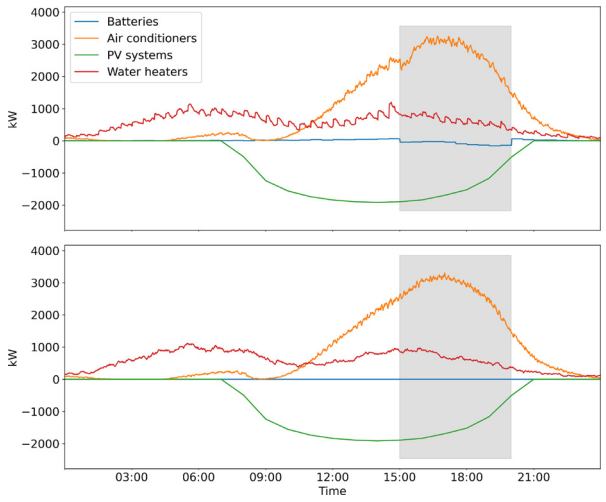

Fig. 14. Comparison of total power of controlled devices in all houses, averaged over the simulated days, for controlled (top) and baseline (bottom) scenarios.

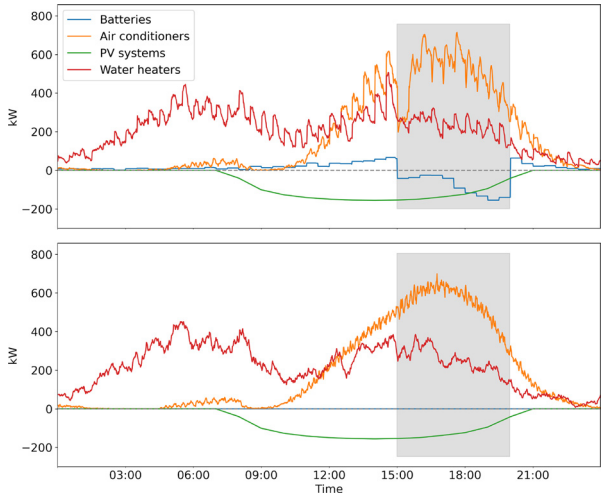

Fig. 15. Comparison of total power of controlled devices in only the homes that are coupled to HEMS in the controlled scenario, averaged over the simulated days, for controlled (top) and baseline (bottom) scenarios.

4.2.2. Simulation results

First, we evaluate the changes in household power consumption and then the changes in the operation of the BESS, water heaters, and air conditioners. We also examine the resulting impact on consumer comfort and system voltages, and, finally, we consider the impact on consumer energy cost.

Figure 11 shows a comparison of the total net power of only the homes that are coupled to a HEMS in the price-responsive—or controlled—scenario, and Fig. 12 shows a comparison of the net power of all homes. The net power differences are further illustrated in Fig. 13. Differences in net power, calculated by subtracting the power for houses with HEMS from the power for houses without HEMS, for each day are shown in light blue, and the differences averaged over all the simulated days are shown in dark blue. For the controlled scenario, the net power increases just before the peak price because the HEMS precools the air and preheats the water, and the net power is decreased during the peak price period, especially at the beginning of the peak price period, compared to the baseline case. The daily net power profile of the homes coupled with HEMS in the controlled scenario have more variability and higher rates of change in power in the controlled scenario than in the baseline scenario, which is a much more demanding electric utility. When comparing all houses in Fig. 12, the differences are less pronounced because only the 20% of homes that are coupled with a HEMS in the controlled scenario behave differently. In addition, because priority is given to homes with BESS and electric water heaters when assigning the HEMS (recall that all homes have air conditioners), a lower percentage of homes that are coupled with HEMS in the controlled scenario have PV systems, so these homes' total net power remains positive at all times, whereas the total net power for all homes is negative when the total PV production exceeds the total load.

Fig. 14 shows the total power of the controllable devices—batteries, air conditioners, and water heaters—and the total PV system output power averaged over all the simulated days for all homes. The top graph is the result for the controlled scenario, and the bottom graph is the baseline result without HEMS and without BESS. Fig. 15 shows the same comparison for only the homes that are coupled with HEMS in the controlled scenario. The HEMS aims to reduce air-conditioning and water heater power consumption, especially during the peak price period, to minimize the consumer-s electricity bill. It achieves this by precooling the air and preheating the water, by allowing the air temperature to rise

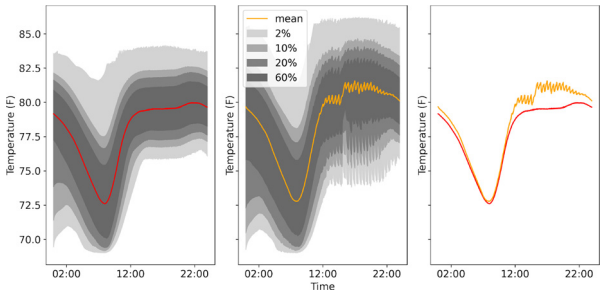

Fig. 16. Comparison of air temperature in only the homes that are coupled to HEMS in the controlled scenario, averaged over the simulated days, with no control (left), with control (middle), and a comparison of average temperatures (right).

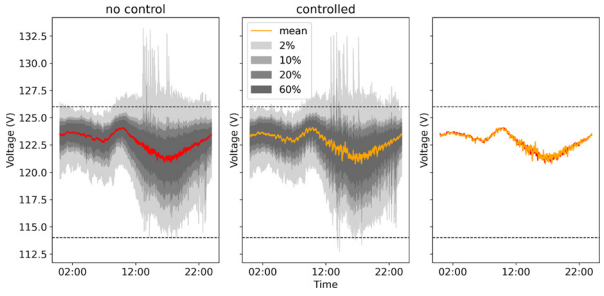

Fig. 17. Comparison of voltages at all homes, averaged over the simulated days, with no control (left), with control (middle), and a comparison of average voltages (right).

above the desired air temperature, and by allowing the water temperature to drop below the desired water temperature. The hot water has a significant draw during the peak price period, which limits the power savings possible. The HEMS schedules the batteries to charge just before and after the peak price period, making use of the PV output, and to discharge during the peak price period to reduce cost to the homeowner.

Fig. 16 compares the air temperatures in homes that have a HEMS coupled in the controlled scenario, and Fig. 17 compares the voltage at all the homes between the baseline and controlled scenarios. In these figures, the graph on the left shows the baseline results with no control, the center graph shows the controlled scenario results, and the graph on the right shows a comparison of averages. In all these graphs, the solid lines display the mean over all 4 days, calculated at 5-minute intervals, and the shaded areas around the solid lines show how the data are distributed as a function of time with the 60%, 20%, 10%, and 2% intervals of the simulated data. The HEMS allows the air temperatures to be higher by up to 2.5°F than the desired air temperatures during and after the peak price period, as shown in Fig. 16, to reduce the air conditioner power consumption. The HEMS precools the air prior to the peak price period to shift power use from times when the cost is higher to earlier hours when it is not as expensive. Because of the high outside temperatures compared to the desired air temperature set points, the air conditioner still needs to operate for most of the peak price period, as shown in Fig. 15.

Figure 17 shows that the feeder's voltage profile is not significantly different between the baseline and the controlled scenarios. The average voltages are slightly higher for the controlled scenario during the peak price period because of the reduction in power drawn by the homes with HEMS during that time. A small percentage of homes experience voltages that exceed the ANSI limits—indicated by the horizontal dotted lines—because of the PV output in both scenarios.

Figure 18 compares the average cumulative cost of electricity for only the homes that are coupled to HEMS in the controlled scenario. As

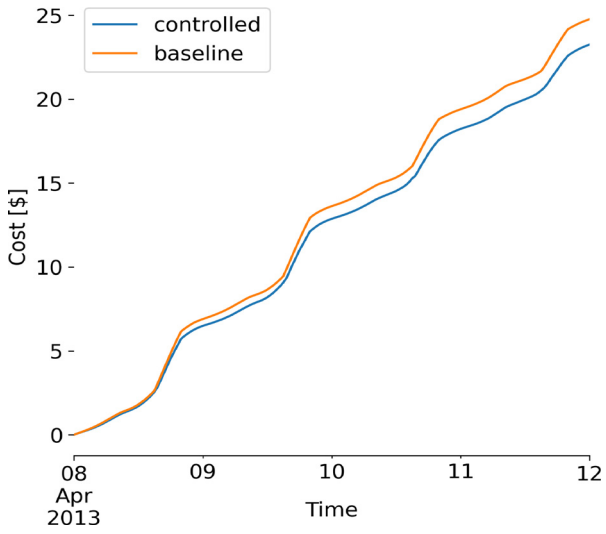

Fig. 18. Comparison of the average cumulative cost of electricity for only the homes that are coupled to HEMS in the controlled scenario in the baseline (orange) and controlled (blue) scenarios. (For interpretation of the references to colour in this figure legend, the reader is referred to the web version of this article.)

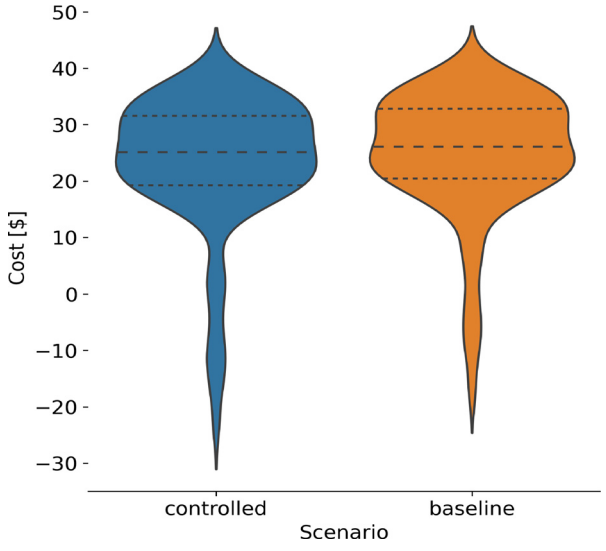

Fig. 19. Comparison of distributions of total cost of electricity for only the homes that are coupled to HEMS in the controlled scenario in the baseline (orange) and controlled (blue) scenarios. (For interpretation of the references to colour in this figure legend, the reader is referred to the web version of this article.)

shown, most of the savings are attained during the peak price period when the HEMS reduces the power drawn from the grid. Fig. 19 shows the distribution of electricity cost for these homes. The costs vary because of variations in the desired air and water temperatures between houses as well as variations in house attributes. For the time period analyzed, the expenses for homes in the controlled scenario are slightly lower than in the baseline scenario—but not statistically significant, and for homes that earn income from the utility, the incomes are higher. This is mainly because these houses take advantage of the credit for exported power during the peak price period by discharging their batteries during that time, as discussed earlier. The average cost is approximately 12% less in the controlled scenario. Fig. 19 compares the cumulative cost of electricity for houses with HEMS.

5. Conclusions

In this paper, we present a stochastic HEMS model that minimizes residential customers' thermal discomfort and energy costs under uncertainty. The HEMS model optimally schedules residential appliances operating in the presence of solar PV within a mixed-integer linear programming. A co-simulation framework is developed to integrate the stochastic HEMS by leveraging the IESM framework to include a larger number of homes on a realistic distribution feeder. Extensive simulations are firstly carried out for a single residential home. The simulation results show the validity of the HEMS model.

The impacts of 1977 homes on an 8,500-node distribution system were simulated. Approximately 25% of the homes had solar panels, and approximately 20% (400 homes) were coupled to a HEMS operating under a TOU rate with net energy metering. The results reported here confirm earlier findings that consumers' electricity costs can be reduced under a TOU tariff if customers invest in BESS and associated controls, such as a HEMS, that can respond to a TOU rate. The HEMS shifts the peak load to off-peak hours, resulting in increased variability and rates of change in power profiles. These results point to both a need for the careful design of tariff structures and to opportunities for aggregator services to coordinate loads and DERs to achieve cost savings for consumers and to gain load profile improvements for utilities. We also studied the impact on the voltage profile across the feeder, and for the scenarios simulated, the impact was not significant.

Future work to evaluate different feeders in different geographic locations can be considered as well as the extension of the HEMS to include faster (second-level) controls with demand response capabilities in addition to the optimization that is performed at intervals of several minutes. Further, a similar impact study can be done under the real-time pricing scheme, in which the electricity price is correlated to both the supply and demand in a distribution market.

Declaration of Competing Interest

The authors declare that they have no known competing financial interests or personal relationships that could have appeared to influence the work reported in this paper.

Acknowledgments

This work was authored in part by the National Renewable Energy Laboratory, operated by Alliance for Sustainable Energy, LLC, for the U.S. Department of Energy (DOE) under Contract No. DE-AC36-08GO28308. Funding provided by U.S. Department of Energy Office of Energy Efficiency and Renewable Energy Office of Strategic Programs. The views expressed in the article do not necessarily represent the views of the DOE or the U.S. Government. The U.S. Government retains and the publisher, by accepting the article for publication, acknowledges that the U.S. Government retains a nonexclusive, paid-up, irrevocable, worldwide license to publish or reproduce the published form of this work, or allow others to do so, for U.S. Government purposes. This work was also supported in part by the U.S. National Science Foundation under Grant No. 1929147 and No. 1856084.

References

[1] IEA. Electricity information: Overview. 2021. Paris, France; https://www.iea.org/reports/electricity-information-overview.
[2] Pratt A, Krishnamurthy D, Ruth M, Wu H, Lunacek M, Vaynshenk P. Transactive home energy management systems: the impact of their proliferation on the electric grid. IEEE Electrif Mag 2016;4(4):8–14. doi:10.1109/MELE.2016.2614188.
[3] A. Brissette, A. Hoke, D. Maksimović and A. Pratt, "A microgrid modeling and simulation platform for system evaluation on a range of time scales," 2011 IEEE Energy Conversion Congress and Exposition, 2011, pp. 968-976, doi:10.1109/ECCE.2011.6063877.
[4] Jo H, Kim S, Joo S. Smart heating and air conditioning scheduling method incorporating customer convenience for home energy management system. IEEE Trans Consum Electron 2013;59(2):316–22. doi:10.1109/TCE.2013.6531112.
[5] Zhao Z, Lee WC, Shin Y, Song K. An optimal power scheduling method for demand response in home energy management system. IEEE Trans Smart Grid 2013;4(3):1391–400. doi:10.1109/TSG.2013.2251018.
[6] Shafie-Khah M, Siano P. A stochastic home energy management system considering satisfaction cost and response fatigue. IEEE Trans Ind Inf 2018;14(2):629–38. doi:10.1109/TII.2017.2728803.
[7] Ahmed MS, Mohamed A, Khatib T, Shareef H, Homod RZ, Ali JA. Real time optimal schedule controller for home energy management system using new binary backtracking search algorithm. Energy Build 2017;138:215–27. doi:10.1016/j.enbuild.2016.12.052.
[8] Wang L. An approximate dynamic programming based home energy management system and its impact on the distribution system. Kansas State University, KS, US; 2019. Master thesis.
[9] Faqiry M, Wang L, Wu H, Krishnamurthy D, Palmintier B. ADP-based home energy management system: A case study using DYNAMO. In: 2018 IEEE Power & Energy Society General Meeting (PESGM); 2018. p. 1–5. doi:10.1109/PESGM.2018.8585796.
[10] Chen S, Liu T, Gao F, Ji J, Xu Z, Qian B, et al. Butler, not servant: a human-centric smart home energy management system. IEEE Commun Mag 2017;55(2):27–33. doi:10.1109/MCOM.2017.1600699CM.
[11] Li H, Wang Z, Hong T, Piette MA. Energy flexibility of residential buildings: asystematic review of characterization and quantification methods and applications. Advances in Applied Energy 2021;3:100054. doi:10.1016/J.ADAPEN.2021.100054.
[12] Mittelviefhaus M, Georges G, Boulouchos K. Electrification of multi-energy hubs under limited electricity supply: de-/centralized investment and operation for cost-effective greenhouse gas mitigation. Advances in Applied Energy 2022;5:100083. doi:10.1016/J.ADAPEN.2022.100083.
[13] Chen Z, Wu L, Fu Y. Real-time price-based demand response management for residential appliances via stochastic optimization and robust optimization. IEEE Trans Smart Grid 2012;3(4):1822–31. doi:10.1109/TSG.2012.2212729.
[14] Wu Z, Zhou S, Li J, Zhang X. Real-time scheduling of residential appliances via conditional risk-at-value. IEEE Trans Smart Grid 2014;5(3):1282–91. doi:10.1109/TSG.2014.2304961.
[15] Chen X, Wei T, Hu S. Uncertainty-aware household appliance scheduling considering dynamic electricity pricing in smart home. IEEE Trans Smart Grid 2013;4(2):932–41. doi:10.1109/TSG.2012.2226065.
[16] Yu Z, Jia L, Murphy-Hoye MC, Pratt A, Tong L. Modeling and stochastic control for home energy management. IEEE Trans Smart Grid 2013;4(4):2244–55. doi:10.1109/TSG.2013.2279171.
[17] Deng R, Yang Z, Chen J, Chow M. Load scheduling with price uncertainty and temporally-coupled constraints in smart grids. IEEE Trans Power Syst 2014;29(6):2823–34. doi:10.1109/TPWRS.2014.2311127.
[18] Albert A, Rajagopal R. Cost-of-service segmentation of energy consumers. IEEE Trans Power Syst 2014;29(6):2795–803. doi:10.1109/TPWRS.2014.2312721.
[19] Mei J, Zuo Y, Lee CH, Wang X, Kirtley JL. Stochastic optimization of multi-energy system operation considering hydrogen-based vehicle applications. Advances in Applied Energy 2021;2:100031. doi:10.1016/J.ADAPEN.2021.100031.
[20] Amabile L, Bresch-Pietri D, Hajje GE, Labbé S, Petit N. Optimizing the self-consumption of residential photovoltaic energy and quantification of the impact of production forecast uncertainties. Advances in Applied Energy 2021;2:100020. doi:10.1016/J.ADAPEN.2021.100020.
[21] Wu H, Pratt A, Chakraborty S. Stochastic optimal scheduling of residential appliances with renewable energy sources. In: 2015 IEEE Power Energy Society General Meeting; 2015. p. 1–5. doi:10.1109/PESGM.2015.7286584.
[22] Liu X, Wu H, Wang L, Faqiry MN. Stochastic home energy management system via approximate dynamic programming. IET Energy Systems Integration 2020;2(4):382–92. doi:10.1049/iet-esi.2020.0060.
[23] Liu X, Wu Y, Zhang H, Wu H. Hourly occupant clothing decisions in residential HVAC energy management. Journal of Building Engineering 2021;40:102708. doi:10.1016/j.jobe.2021.102708.
[24] Rahmani-Andebili M. Scheduling deferrable appliances and energy resources of a smart home applying multi-time scale stochastic model predictive control. Sustainable Cities and Society 2017;32:338–47. doi:10.1016/j.scs.2017.04.006.
[25] Ruth M, Pratt A, Lunacek M, Mittal S, Wu H, Jones W. Effects of home energy management systems on distribution utilities and feeders under various market structures. In: 23rd International Conference on Electricity Distribution; 2015. p. 1560–5.
[26] Pratt A, Banerjee B, Nemarundwe T. Proof-of-concept home energy management system autonomously controlling space heating. In: 2013 IEEE Power Energy Society General Meeting; 2013. p. 1–5. doi:10.1109/PESMG.2013.6672709.
[27] Edwards W, Barron F. Smarts and smarter: improved simple methods for multiattribute utility measurement. Organ Behav Hum Decis Process 1994;60(3):306–25. doi:10.1006/obhd.1994.1087.
[28] Hoke A, Brissette A, Smith K, Pratt A, Maksimovic D. Accounting for lithium-ion battery degradation in electric vehicle charging optimization. IEEE J Emerg Sel Top Power Electron 2014;2(3):691–700. doi:10.1109/JESTPE.2014.2315961.
[29] Boone A. Simulation of short-term wind speed forecast errors using a multi-variate ARMA(1,1) time-series model. KTH, Stockholm, Sweden; 2005.
[30] Guan X, Xu Z, Jia Q. Energy-efficient buildings facilitated by microgrid. IEEE Trans Smart Grid 2010;1(3):243–52. doi:10.1109/TSG.2010.2083705.
[31] Khodayar ME, Shahidehpour M, Wu L. Enhancing the dispatchability of variable wind generation by coordination with pumped-storage hydro units in stochastic power systems. IEEE Trans Power Syst 2013;28(3):2808–18. doi:10.1109/TPWRS.2013.2242099.
[32] Dupačová J, Gröwe-Kuska N, Römisch W. Scenario reduction in stochastic programming. Math Program 2003;95(3):493–511. doi:10.1007/s10107-002-0331-0.
[33] GridLAB-D simulation software. 2021a. https://www.gridlabd.org/.

[34] Pratt A, Ruth M, Krishnamurthy D, Sparn B, Lunacek M, Jones W, et al. Hardware-in-the-loop simulation of a distribution system with air conditioners under model predictive control. In: 2017 IEEE Power & Energy Society General Meeting. IEEE; 2017. p. 1–5. doi:10.1109/PESGM.2017.8273757.

[35] PG&E-s time-of-use rate plans. 2021b. https://www.pge.com/en_US/residential/rate-plans/rate-plan-options/time-of-use-base-plan/time-of-use-plan.page.

[36] Holmberg D, Burns M, Bushby S, Gopstein A, McDermott T, Tang Y, Huang Q, Pratt A, Ruth M, Ding F, Bichpuriya Y, Rajagopal N, Ilic M, Jaddivada R, Neema H. NIST transactive energy modeling and simulation challenge phase II final report. Tech. Rep.. National Institute of Standards and Technology; 2019. doi:106028/NISTSP1900-603.

[37] Pacific Northwest National Laboratory. Transactive energy simulation platform (TESP). 2021. https://github.com/pnnl/tesp/blob/b01db4b26b2d4e9f9462a4ff241e3ba6bfb12955/examples/ieee8500/IEEE_8500gener_whouses.m.

[38] Renewable energy riders. 2021c. https://www.aps.com/en/Residential/Service-Plans/Compare-Service-Plans/Renewable-Energy-Riders.